

Design and Implementation of Flyback Converter for Electrical Discharge Machining Power Generator

Nazriah Mahmud^a, Azli Yahya^{a*}, Trias Andromeda^b, Nor Liyana Safura Hashim^a

^aFaculty of Biosciences and Medical Engineering, Universiti Teknologi Malaysia, 81310 UTM Johor Bahru, Johor, Malaysia

^bFaculty of Electrical Engineering, Universiti Teknologi Malaysia, 81310 UTM Johor Bahru, Johor, Malaysia

*Corresponding author: azli@fke.utm.my

Article history

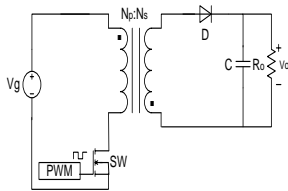
Received :23 October 2013

Received in revised form :

14 December 2013

Accepted :10 January 2014

Graphical abstract



Abstract

Electrical Discharge Machining process has been widely used for manufacturing micro components due to its contactless process. Its application has also been introduced in machining micro pits on hip implant. In this paper, a new design of power generator is proposed in order to reduce micro crack while machining take place. Flyback Switch Mode Power Supply has been chosen because of its high efficiency. The simulation of Flyback converter using LT Spice is presented. The result shows that the system achieves 95.9% of efficiency. Experimental results show that flyback converter able to produce DC voltage up to 111.6 V.

Keywords: Flyback; electrical discharge machining

Abstrak

Pemesinan nyah cas elektrik telah digunakan secara meluas bagi pembuatan komponen mikro disebabkan oleh proses tanpa sentuh itu. Penggunaannya juga telah diperkenalkan dalam pemesinan lubang mikro pada implan pinggul. Dalam kertas ini, reka bentuk baru penjanakuasa adalah dicadangkan untuk mengurangkan retak mikro semasa proses pemesinan berlaku. Bekalan kuasa mod suis telah dipilih kerana kecekapan yang tinggi. Simulasi Flyback menggunakan LT Spice dibentangkan. Hasilnya menunjukkan bahawa sistem itu mencapai kecekapan sebanyak 95.9%. Hasil eksperimen menunjukkan flyback mampu menghasilkan voltan arus terus sebanyak 111.6 volt.

Kata kunci: Pemesinan nyah cas elektrik; flyback

© 2014 Penerbit UTM Press. All rights reserved.

1.0 INTRODUCTION

Hip joint is a congruous joint where acetabulum (concave) and the femoral head (convex) are symmetrical. It is held firmly by a thick capsule that contain a synovial fluid (SF), a biological lubricant that acts like a shock absorber.¹ The femoral head is coated by a cartilage that serves as cushion and lubricates the joint during compression as well as to accommodate the full range of motion.² Unfortunately, the hip joint is prone to degenerate due to any causes such as chronic disease, malformation of the hip since birth, damaged from injury or in aged people. The best clinical solution is the hip arthroplasty, a surgical technique that replaces the unhealthy hip joint with an implant.³

However, there are two main critical issues arise in metal-on-metal hip implant: the loosening of implants due to implant and bone interaction and wear of articulating surface (femoral head).⁴ One of the way to minimize wear is through improving

lubrication activities by changing surface topography or surface texture.⁵ This approach can be accomplished by applying micro pits on the metallic acetabular cup, which help to promote retention of lubricant between the contact surfaces.⁶

Micro pits are also reported able to act as fluid reservoir as well as to avoid the abnormal temperature rise caused by dry running conditions.⁶ Direct contact from tool to workpiece for creating micro pits would not be the best solution because it suffers from micro crack due to drilling and stamping process. However, contact-less process, which is a characteristic of an Electrical Discharge Machining (EDM) process, make it capable to machine micro pits with minimal surface crack and improving material removal rate. These micro pits will be act as the reservoir of lubricant as well as improve friction between contact surfaces. In commercial EDM system⁷, a voltage up to 200 Volt and currents up to 150 Amperes is applied to interelectrode gap. A study by Hasçalik and Caydaş⁸ reported that surface cracks density is wider as pulse current increases

while Prabhu and Vinayagam⁹ stated that the micro crack depth is expanding with increasing pulse currents. A report by A.Yahya¹⁰ shows that material removal rate also will be improve with low gap current.

Therefore, for machining micro pits on the metallic acetabular cup, a particular design of Pulse Power Generator (PPG) would be developed in an attempt to find the appropriate machining parameters. Flyback Switch Mode Power Supplies (SMPS) will be implemented in designing the new PPG. This is because; the output power level required is less than 150 Watt, which make the design of power transformer is relatively simple. In addition, only one magnetic element (flyback transformer) is used as inductors are not required in the output filter. It also has wide input voltage range as well as multiple outputs can be obtained using a minimum number of parts.

This paper presents simulation of flyback SMPS using LT Spice. The paper is organized as follows; Section 2 discusses the flyback converter and its mathematical representation. Section 3 covers the simulation model and experimental set up, Section 4 presents the simulation and experimental results and Section 5 concludes this paper.

2.0 FLYBACK CONVERTER

One of the key elements of EDM is a power generator unit that controls the amount of energy consumed. This power generator helps to maintain the machining gap (known as spark gap) in order to generate succession of uniform electrical discharge in the form of sparks. It has a time-control function, which called on time that control the length of time that current flows each pulse. It also controls the amount of current allowed to flow during each pulse. In conventional EDM, the voltage and current level are high, thus the electrode gets locally melted and welded workpiece and electrode.¹¹ Moreover, a present of stray arching should be minimized or eliminated. Until now, a number of power supply units have been developed ranging from basic resistance-capacitance (RC) power supply to the complex resonant power supply unit. The Pulse Power Generator (PPG) is a critical section of EDM system for achieving the required parameter of accuracy, smooth surface finish and size of micro machining through an EDM process. A Relaxation-type RC pulse power supply is the earliest pulse power for EDM, with simple structure and reliable capability, is able to generate a small pulse width of narrow pulse. However, the pulse in the discharge process is uncontrollable. The machined parts would suffer from micro crack; melted electrode and left over debris. Machining micro-pits using new design of PPG using microcontroller chip to control the pulse generation, will overcome the drawback of the commercial PPG. Furthermore, some energy-saving EDM pulse power supplies have replaced the existing linear power supplies.¹²⁻¹³ Thus, in this project pulse power generator will be designed by implementing Switch Mode Power Supplies which is flyback converter.

Figure 1 illustrated the application of the power generator in EDM system. The power generator will be applied between the electrode and workpiece (hip implant). The machined micro pits are expected to be free from micro crack with improving material removal rate.

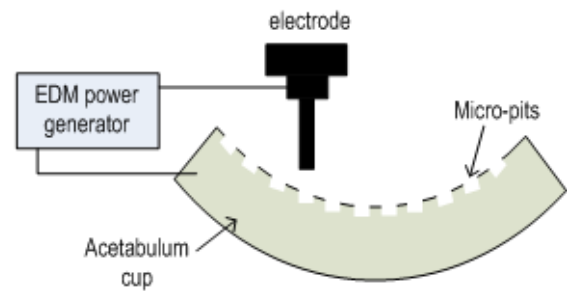


Figure 1 Micro pits machined with good surface finish

Figure 2 shows the flyback converter topology with Pulse Width Modulation (PWM) as the switching controller.

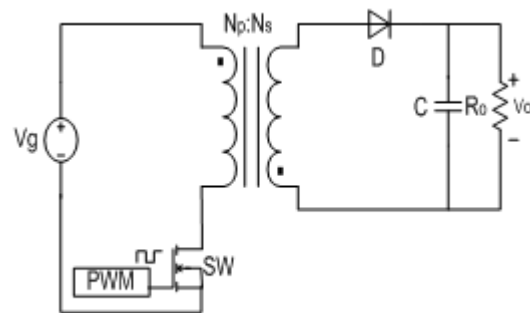


Figure 2 Flyback converter topology

Here, power MOSFET is chosen because it switches five to ten times faster and easier to be used in a design. Flyback converter operation is divided when switch (SW) is on and when switch (SW) is off. The mathematical representation of both conditions in¹⁴ is discussed. There are two possible modes of operation for Flyback SMPS: Discontinuous Conduction Mode (DCM) and Continuous Conduction Mode (CCM).¹⁵ In DCM, all energy stored in the inductor is transferred to an output capacitor and load circuit before another charging period occurs. While in CCM, energy stored in the inductor not completely transferred.

In the DCM, the circuit topology results in a smaller inductor but put larger stress on the capacitor and switching device. Therefore, the winding losses increased due to the higher rms value of higher peak currents. Higher ripple current and ripple voltage in the input and output capacitor, gives added stress to the switching transistor. However, the advantage of this circuit is when the switching device is turned on, the initial current is zero. This means the output diode has completely recovered which reduce the EMI radiation. Besides, the DCM does not exhibit the right half plane zero which make the loop is easy to control. Thus, DCM is implemented and discussed in this simulation.

2.1 When Switch Is On

Figure 3 shows a parasitic-elements-free flyback when switch (SW) is closed. The primary of the transformer is directly

connected to the input voltage. Thus, the voltage across the primary inductor L_p is equal to the input voltage. During this time, there is no current flowing in the secondary side inductor. During the on time, the diode anode swing negative, thus blocking the current from circulating in the secondary side. The output capacitor supplies energy to the output load.

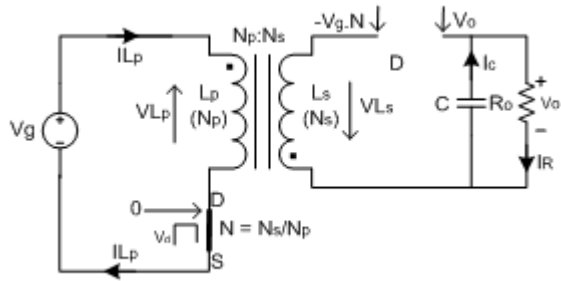


Figure 3 Flyback converter during on time

2.2 When Switch Is Off

Figure 4 shows a parasitic-elements-free flyback when switch (SW) is opened. When the switch is turned off, the voltage across the primary inductor reverses, in an attempt to keep the ampere-turns constant. However, as the secondary diode now senses a positive voltage on its anode, allowing current to flow from the transformer. The secondary-side-transformer terminal is now biased to the output voltage, V_{out} , by neglecting the diode forward drop. The energy from the transformer core recharges the capacitor and supplies the load.

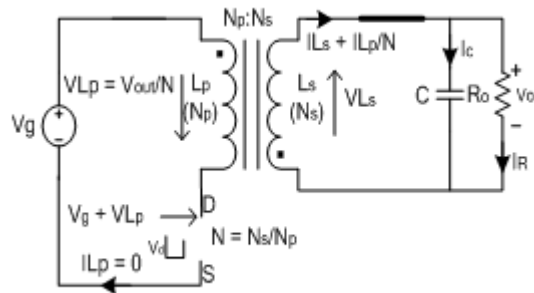


Figure 4 Flyback converter during off time

2.3 Mathematical Representation

During on time, the current in the primary inductor increase at a rate defined by

$$S_{on} = V_g/L_p \tag{1}$$

Considering the on time, t_{on} and the valley current, I_{valley} , Equation 1 can be updated to define the peak current value

$$I_{peak} = I_{valley} + (V_g/L_p)t_{on} \tag{2}$$

Here, I_{valley} represents the initial inductor current condition for

$t = 0$ (if in CCM). As for the DCM, I_{valley} is zero.

$$I_{peak} = (V_g/L_p)t_{on} \tag{3}$$

At this time, the diode swing negative, thus blocking the current from flowing in the secondary side inductor. Due to the capacitor presence, the peak inverse voltage (PIV) undergone by the rectifier is simply

$$PIV = V_g N + V_o \tag{4}$$

Where N is the turns ratio linking both inductors, equal to

$$N = N_s/N_p \tag{5}$$

When the PWM controller instructs the power switch to turn off, the voltage across the primary inductor suddenly reverses, in an attempt to keep the ampere-turns constant. The upper switch terminal voltage quickly jumps to

$$V_{DS,off} = V_g + VL_p \tag{6}$$

However, the diode now senses a positive voltage on its anode, it can conduct.

$$V_{DS,off} = V_g + V_o (N_p/N_s) = V_g + V_o/N \tag{7}$$

The voltage applied across the inductor now being negative, it contributes to reset the core magnetic activity. The rate at which reset occurs is given by

$$S_{off} = -(V_o/NL_p) \tag{8}$$

By introducing the off-time, Equation 7 can be updated to extract the valley current if the flyback operates in CCM:

$$I_{valley} = I_{peak} - (V_o/NL_p)t_{off} \tag{9}$$

Since in DCM, $I_{valley} = 0$, Equation 7 can be updated and become:

$$I_{peak} = (V_o/NL_p)t_{off} \tag{10}$$

Combining Equation 3 and Equation 9

$$(V_o/NL_p)t_{off} = (V_g/L_p)t_{on} \tag{11}$$

Expressing the duty cycle, D in relation to the on and off times, the final definition for CCM is:

$$V_o/V_g = N t_{on}/t_{off} = N D T_{sw}/(1-D) T_{sw}$$

$$V_o/V_g = ND/(1-D) \tag{12}$$

The output power;

$$P_{out} = (1/2) I_{peak}^2 L_p F_{sw} \eta \tag{13}$$

For output filter capacitor;

$$C_{out(min)} = (I_{out(max)} - (1 - D_{(min)}) f) / f * V_{ripple(pk-pk)} \tag{14}$$

Where:

I_{out} : rated output current

$D_{(min)}$: smallest estimated duty cycle
 $V_{ripple(pk-pk)}$: the desired peak to peak output ripple voltage

3.0 DESIGN AND IMPLEMENTATION

3.1 Simulation Design

From the mathematical representation derived in section II, the parameters used in this simulation are discussed in Table 1 below. The purpose of this simulation is to calculate the efficiency of the flyback converter.

Table 1 Parameters used

Parameter used	Value
Input voltage, V_g	340 V
Switching frequency, F_{sw}	100 kHz
On time, t_{on}	3 μ s
Off time, t_{off}	7 μ s

From the derived equation, by assuming the converter efficiency, η is 80%

- i) Primary inductance, $L_p = 416 \mu$ Henry is calculated from:

$$L_p = 2P_{out} / (I_{peak}^2 F_{sw} \eta) \tag{15}$$
- ii) Winding ratio, $N = 0.7$
- iii) Primary peak current, $I_{peak} = 2.45$ A

Based on parameters described, a simulation is conducted. Figure 5 shows the flyback converter design in LT Spice environment with 100 Ω of resistance is used as the load.

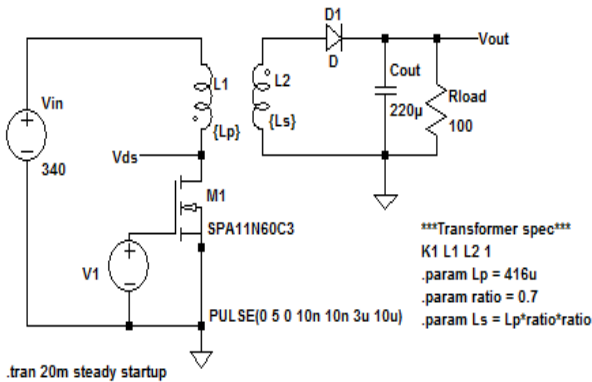


Figure 5 Flyback converter design in LTSpice

3.2 Hardware Implementation

After a simulation has been conducted, an experiment is carried out to verify the performance of the flyback converter. Figure 6 depicts the schematic diagram of open loop flyback converter used in the experiment. For switching method, commercial Pulse Width Modulator (PWM) IC's has been used namely UC3842. This IC provides good electrical performance in current mode operation with minimal cost. It is optimized for

power sequencing of off-line converter, DC to DC regulators and for driving power MOSFETs or transistor. Figure 7 shows the experimental set up to test the flyback converter. The experiment is done by varying the load value.

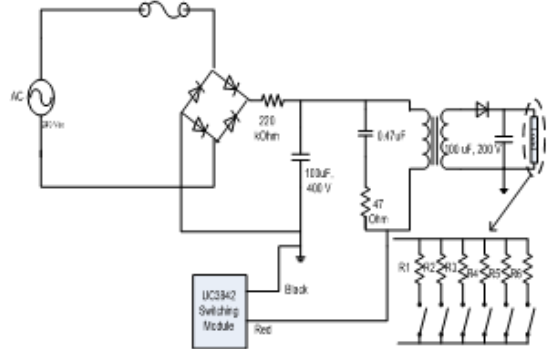


Figure 6 Schematic diagram of open loop flyback converter with UC3842 as the switching module

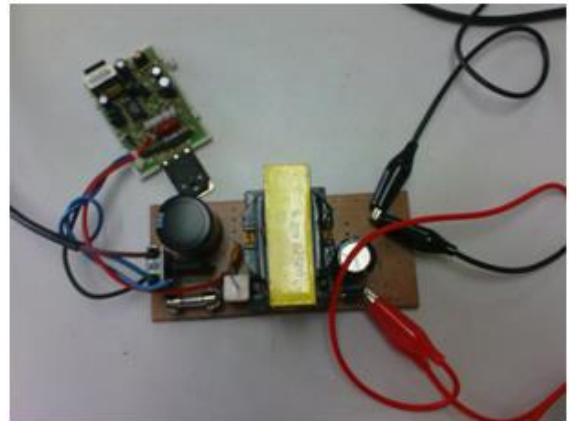


Figure 7 Flyback converter with UC3842 as switching module

4.0 RESULT AND DISCUSSION

4.1 Simulation Result

Pulse Width Modulation (PWM) switching controller can take in different forms, where pulse frequency is one of the most important parameters when defining a PWM method. It can be either constant or variable.¹⁶ For this simulation, a Constant-Frequency (CF) PWM is used as depicted in Figure 8 (first graph). The on and off time is kept constant from the beginning to the end of simulation.

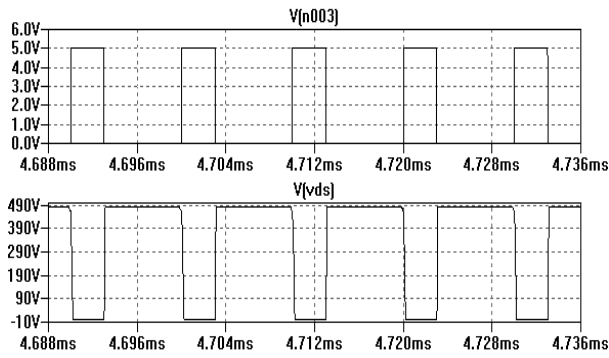


Figure 8 Pulse width modulation (PWM) waveform and V_{ds}

Since the flyback converter works in DCM, it allows valley current to reach zero. Figure 9 illustrated the current waveform during DCM operation. The primary inductor current (second graph) shows that the energy in the inductor is fully transferred to the output capacitor and load before another charging period occur.

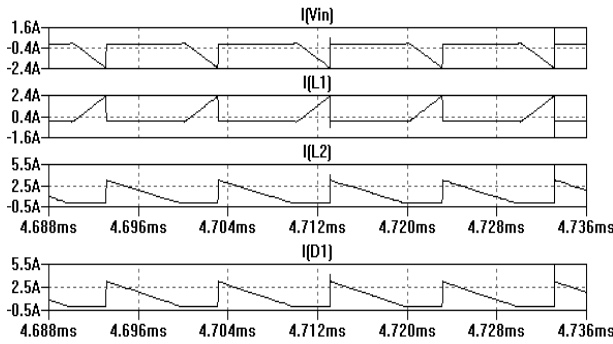


Figure 9 The current waveform of flyback converter during DCM

Figure 10 shows the output voltage (V_{out}) and output current (I_{Rload}). As the voltage climbs up to 100 Volt and current climbs up to 1 Amperes, the output is regulated and maintain that value. From this simulation results shows that the designed flyback converter able to supplies 100 Volt voltage and 1 Amperes current to the EDM system.

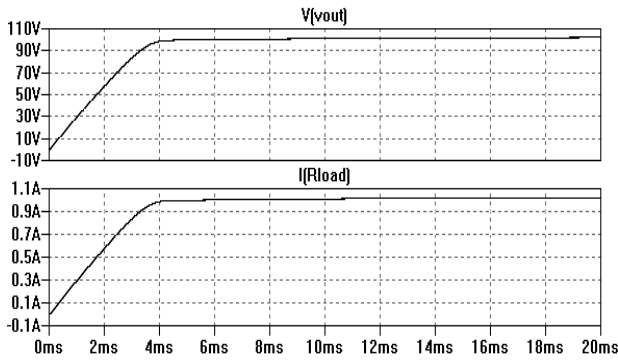


Figure 10 Output voltage and output current

For 20 ms of time simulation, average output voltage and output current obtained is 92.018 Volt and 0.92 Amperes respectively.

Table 2 shows the power dissipation in the individual components of the proposed designed. The simulation result shows that the design achieves 95.9% of efficiency. The efficiency is calculated based on:

$$\text{Efficiency} = (P_{out}/P_{in}) * 100 \tag{16}$$

From the simulation:

P_{out} : 104 Watt, P_{in} : 108.4 Watt ; thus efficiency = 95.9%

Table 2 Efficiency report

Ref.	Irms(mA)	Ipeak(mA)	Power dissipation(mW)
Cout	1069	2815	0
D1	1494	3836	885
L1	705	2272	0
L2	1494	3836	0
M1	705	2272	3601

4.2 Experimental Result

Figure 11 displays the input voltage waveform. It is a DC input voltage with peak to peak value of 356 Volt with 100 V/div. In order to evaluate the capability of the flyback converter, different value of load has been given to the output terminal. Table 3 describes the measured value of output current, output voltage, and resistance. From the table shows that flyback converter able to produce a DC output voltage up to 111.6 Volt and output current up to 0.99Amperes.

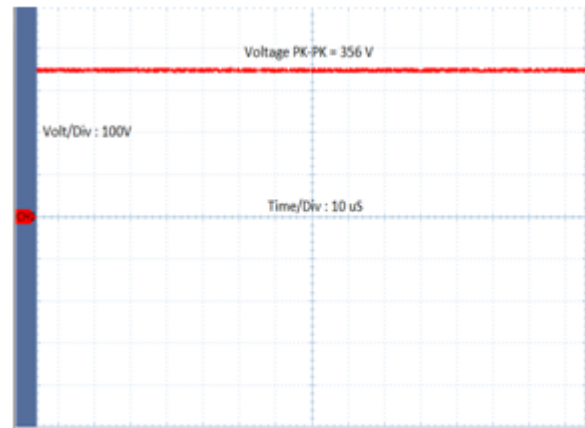
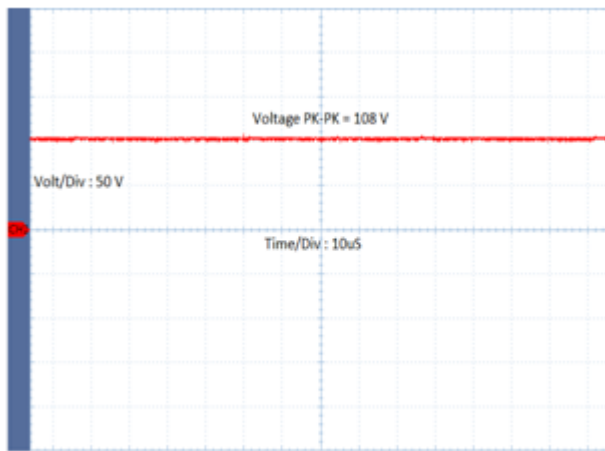


Figure 11 Input voltage waveform

Table 3 Experimental results by varying the value of load

Resistance (Ω)	Output Current (A)	Output Voltage (V)
1014.5	0.11	111.6
477.1	0.21	100.2
379.2	0.26	98.6
312.3	0.31	96.8
184.3	0.51	94.0
155.0	0.60	93.0
122.9	0.75	92.2
92.1	0.99	91.2

Figure 12 shows the output voltage waveform captured using oscilloscope when load is 477.1 Ω . The peak to peak voltage is 108V with 50 volts/div. From the experimental result shows that the designed flyback converter can be used for machining micro pits on the hip implant since the output voltage and output current can be varied by using resistor as its limiter.

**Figure 12** Output voltage waveform when load is 477.1 Ω

5.0 CONCLUSION

EDM has become one of the most effective methods of machining materials of any hardness as long as the material is an electrically conductive. For proper good machining

condition, high material removal rate and good surface finish is demanded. In this paper, an efficient power generator for machining micro pits on hip implant is discussed. A flyback SMPS has been suggested for the new power generator design. The result from simulation shows that flyback SMPS is recommended due to the low power application and also its high efficiency. Experimental result shows that the designed flyback converter able to produce a DC output voltage up to 111.6 Volt.

Acknowledgement

Authors would like express deepest gratitude to the Research Management Center (RMC), Universiti Teknologi Malaysia for their financial support.

References

- [1] M. Nordin, V. H. Frankel. 2001. *Basic Biomechanics of the Musculoskeletal System*. Philadelphia, PA :Lippincott Williams & Wilkins.
- [2] D. P. Byme, K. J. Mulhall, and Baker, J. F. 2010. *The Open Sports Medicine Journal*. 4: 51–57.
- [3] A. Rabiei. 2009. *Hip Prosthesis*, in *Biomedical Material*. R. Narayan, Editor. 2009, Springer US. 349–369.
- [4] L. Mattei, F. Di Puccio, et al. 2011. *Tribology International*. 44: 532–549.
- [5] L. Gao, P. Yang, et al. 2010. *Tribology International*. 43: 1851–1860.
- [6] M. Wakuda, Y. Yamauchi, et al. 2003. *Wear*. 254: 356–363.
- [7] L. I. Sharakhovskiy, A. Maotta, and Essiptchouk, A. M. 2006. *Applied Surface Science*. 253: 797–804.
- [8] A. Haşçalık and U. Çaydaş. 2007. *Applied Surface Science*. 253: 9007–9016.
- [9] S. Prabhu and Vinayagam, B. K. 2010. *IACSIT International Journal of Engineering and Technology*. 2: 35–41.
- [10] A. Yahya and C. D. Manning. 2004. *J. Phys. D: Appl. Phys.* 37: 1467–1471.
- [11] M. Kunieda, B. Lauwers, et al. 2005. *CIRP Annals-Manufacturing Technology*. 54: 64–87.
- [12] S. C. Di, D. B. Wei, et al. 2006. *Key Engineering Materials*. 315–316:516–520.
- [13] Y. K. Wang, Z. L. Wang, et al. 2010. *Key Engineering Materials*. 447–448: 247–252.
- [14] C. Basso. 2008. *Simulations and Practical Designs of Flyback Converters*. New York, Chicago, San Francisco, Lisbon, London, Madrid, Mexico City, Milan, New Delhi, San Juan, Seoul, Singapore, Sydney, Toronto.
- [15] McLyman, C. W. T. 2004. *Transformer and Inductor Design Handbook*. M.O. Thurston.
- [16] J. Sun. 2012. *Pulse-Width Modulation*. In *Dynamics and Control of Switched Electronic Systems*.